ARTICLES

Pion absorption by ^{3}He at the Δ-resonance energy

S. Mukhopadhyay, S. Levenson,* R. E. Segel, and G. Garino
Northwestern University, Evanston, Illinois 60201

D. Geesaman, J. P. Schiffer, G. Stephans,† B. Zeidman, E. Ungricht, H. Jackson, and R. Kowalczyk
Physics Division, Argonne National Laboratory, Argonne, Illinois 60439

D. Ashery, E. Piasetsky, M. Moinester, and I. Navon
Department of Physics, Tel-Aviv University, Ramat Aviv, Israel 69978

L. C. Smith, R. C. Minehart, G. S. Das, and R. R. Whitney
Department of Physics, University of Virginia, Charlottesville, Virginia 22901

R. Mckeown
Department of Physics, California Institute of Technology, Pasadena, California 91125

B. Anderson, R. Madey, and J. Watson
Kent State University, Kent, Ohio 44242
(Received 29 October 1990)

Pion absorption by ^{3}He was studied at $T_\pi = 165$ MeV in a kinematically complete experiment. The cross section for absorption on a (pn) pair of nucleons, $\sigma_{pn}(\pi^+)$, was found to be 17.0 ± 2.6 mb; that for absorption on a (pp) pair, $\sigma_{pp}(\pi^-)$, 0.91 ± 0.20 mb. The angular distribution in the πNN center-of-mass system for $\sigma_{pn}(\pi^+)$ resembles that for the $\pi^+ + d \rightarrow p + p$ reaction while the angular distribution for $\sigma_{pp}(\pi^-)$ is strongly backward peaked. Evidence that a significant fraction of the absorptions involves all three target nucleons is seen in the angular correlation between the two detected nucleons as well as in the momentum distribution of the unobserved nucleon. For π^+ and π^- absorption, the three-body cross sections were found to be 9.6 ± 2.1 and 4.2 ± 01.2 mb, respectively. Neither initial- nor final-state interactions appear to be major contributors to the observed three-body absorption, though initial-state interactions may be contributing to the enhancement of the three-body π^+ absorption at the Δ resonance.

I. INTRODUCTION

The experimental study of pion absorption in nuclei is important in understanding the nucleon-nucleon interaction, as well as the interaction of pions with nuclei. Studies of pion absorption on the deuteron,[1,2] a $T=0$, $J=1$ system, are not sufficient to describe absorption in nuclei that contain more nucleons as well as other isospin and angular-momentum couplings. The ^{3}He nucleus allows for a comparative study of absorption on $T=0$, $J=1$ and $T=1$, $J=0$ nucleon pairs. The present experiment studied the kinematically complete reactions $^3\mathrm{He}(\pi^+, pp)$ and $^3\mathrm{He}(\pi^-, pn)$ at $T_\pi + 165$ MeV.

Pion absorption on ^{3}He, which has a central density similar to that of heavier nuclei, rather than the comparatively low density of the deuteron, may be more pertinent to absorption in heavier nuclei. Previous pion absorption studies on a range of nuclei[3,4] suggest that the quasideuteron absorption mechanism is not the predominant process. In ^{3}He, some insight into the behavior of other processes may be gained through measurements in regions of phase space that are away from the two-body peak.

Previous studies of this reaction were carried out for stopped pions,[5] and at $T_\pi = 62.5$,[6,7] 64,[8] 82.8,[6], 119,[8,9] 162,[8] 165,[10] 206,[8], and 500 MeV,[11] measuring two outgoing nucleons in coincidence. Singles measurements have been made at various energies between 50 and 295 MeV.[12] In experiments performed at energies at or below the Δ resonance, it was found that (1) the nucleons from pion absorption on a $T=0$, $^3S_1$ pair have an angular distribution very similar to that from absorption on a deuteron with a normalization factor of about 1.5, (2) negative pion absorption on a $T=1$, $^1S_0$ pair is an order of magnitude weaker than on the deuteron with the Δ resonance not playing a major role in this channel, and (3) the cross

section for absorption processes in which all three nucleons share the energy is about half that of two-nucleon absorption.

II. EXPERIMENT

The experiment was performed at the P^3 East channel at LAMPF. Figure 1 shows the plan view of the experimental setup. All pion absorption data were taken with the channel set for a momentum spread of $\pm 1\%$. Typical fluxes were 5×10^7/sec for π^+ and 10^7/sec for π^-. The proton beam was monitored by a toroid counter that integrated the beam and by an ionization chamber that monitored the radiation coming from the production target; the ratio of these two monitors remained constant to within about 1%. The pion flux was monitored by telescopes, mounted on either side of the pion beam as it entered the experimental area, which counted muons from π-μ decay. The pion beam was also monitored by an ionization chamber which intercepted the beam downstream of the target. Absolute measurements of the pion flux were made by counting the ^{11}C activity from a carbon target using the $\pi^{\pm}(^{12}\mathrm{C},n)^{11}\mathrm{C}$ cross sections as standards.[13]

The target was a cylindrical cell of liquid ^{3}He maintained at a temperature of 1.5 K. Details of the target cell and associated cryostat are given elsewhere.[14] The target density was held constant to $\pm 1\%$, as determined by measurements of the ^{3}He vapor pressure. The number of interactions was also dependent on the beam profile but, by measuring the profile on a Polaroid film and by employing a beam profile monitor, it was possible to determine the effective target thickness to $\pm 6\%$. A target cell identical to the one that was used, except that the walls were a factor of 4 thicker, was run empty for background measurements.

Proton momenta were measured by the Large Acceptance Spectrometer (LAS), which is described in detail elsewhere.[15] Momenta were determined by measuring the angular deflection of the particles as they passed through the dipole magnet. The incident and emergent angles were determined from pairs of multiwire proportional chambers at both the entrance and the exit of the spectrometer. The acceptance range was about $0.80 < p/p_0 < 1.40$ with $p_0 = 750$ MeV/c the maximum attainable. An acceptance scan was taken by measuring the yield as a function of magnetic field of protons from the $\pi^+ + d \rightarrow p + p$ reaction. With these same protons, the momentum resolution was determined to be about 1.5%. The solid angle was about 5.3 msr in the first phase of the experiment and about 2.4 msr in the second. It is possible for LAS to subtend a much larger solid an-

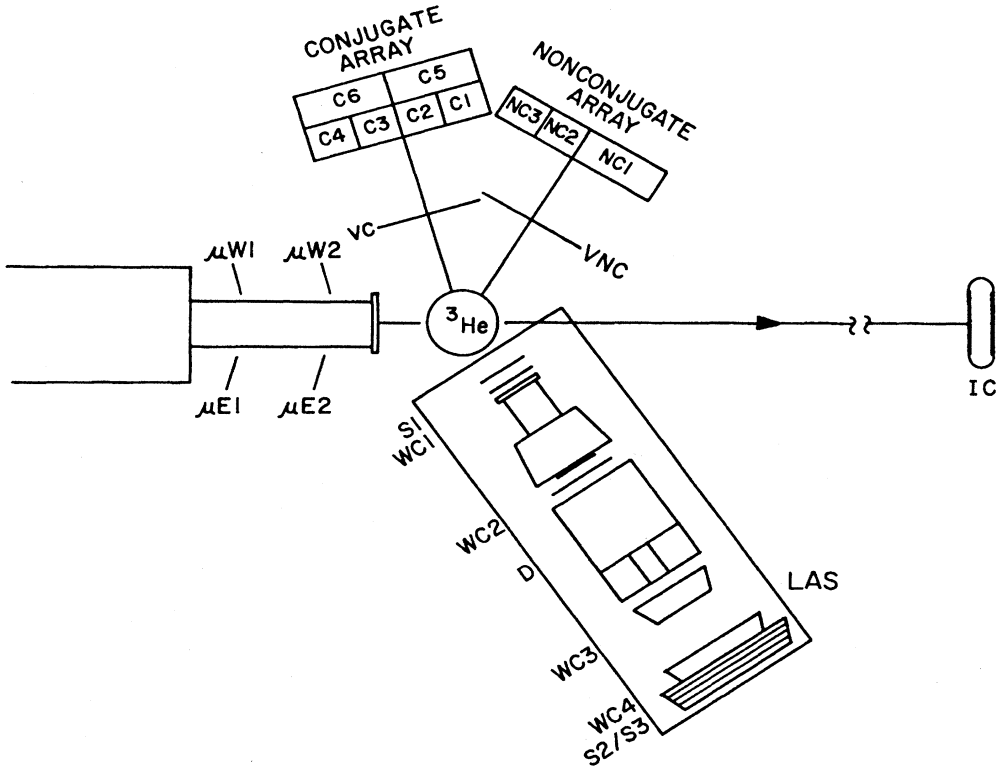

FIG. 1. A top view of the experimental setup. In LAS, counters labeled S are scintillators and those labeled WC are wire chambers, while D denotes dipole. Counters labeled μ are muon counters, which monitored the pion flux.

gle, ~25 msr, but, in order to extend the angular and momentum ranges, the quadrupole doublet was removed and the first wire chamber moved farther from the target.

A coincidence between the plastic scintillator at the entrance $S1$ and the two arrays of plastic scintillator at the exit $S2$ and $S3$ provided the LAS event. All detectors in the system were timed relative to $S1$.

The efficiency of each plane of wire chambers was determined from the ratio of the number of events in which all but that plane fired to the number of events when all planes fired. Each wire chamber was usually >95% efficient and the overall efficiency of the wire chamber system was typically about 75%. The LAS deadtime was measured by comparing the total number of LAS events to the number voted by a fast inhibit which was reset when the event processing was finished. Typical LAS deadtimes were 5–8 %. It should be noted that the LAS deadtime was distinct from the computer busy deadtime, which was measured separately and duly allowed for.

The LAS solid angle was determined by measuring the yield, at three angles, of the $\pi^+ + d \rightarrow p + p$ reaction. The cross section for this reaction is known to a few percent. These three determinations of the solid angle agreed to ±5%. The normalization was checked by measuring the $\pi^+ p$ scattering cross section, which was found to be within 7% of the accepted value. Overall, it is estimated that the cross sections quoted in the present work have an absolute systematic error of ±15%.

A coincident nucleon, proton for π^+ absorption and neutron for π^-, was detected in one of two large arrays of plastic NE-102 scintillators. One array was composed of four bars ($C1$, $C2$, $C3$, $C4$), each 10 cm×25 cm×1 m, backed by two 10 cm×50 cm×1 m bars ($C5$, $C6$) while the other consisted of a single layer which contained two 10 cm×25 cm×1 m bars ($NC2$, $NC3$) and one 10 cm×50 cm×1 m bar ($NC1$). The front face of the forward bars was 2 m from the target and, therefore, each array subtended an angle of ±14° in both the horizontal and vertical directions. For each angular setting of LAS one array (usually the one with a double row of bars) was centered at the angle where the other nucleon from $\pi + d \rightarrow N + N$ would be present. This array was called the "conjugate" array and the other array, referred to as the "nonconjugate" array, was centered 30°–40° away. When protons were detected, the back row of the double-layered array was used for particle identification only.

The two ends of each bar were attached to plastic light pipes which were tapered down to meet a 12.7-cm photomultiplier tube. A time resolution of about 250 psec was achieved using the mean-timing technique, while the position of an event could be determined to ±2.5 cm from the time difference between signals reaching the opposite ends of a bar. As discussed in more detail below, this position information was very useful in making the kinematically complete reconstructions. A coincidence between the two ends of any bar provided the bar event trigger which, in coincidence with a Las event, provided the master trigger. The gains of all of the photomultiplier tubes were set to be approximately equal and, in the analysis, a software threshold of 6±2-MeV equivalent electron energy was set on all of the tubes. The pulse-height spectrum from each tube was monitored and the stated uncertainty in the threshold allows for gain drifts.

The neutron efficiency of the bars was calculated by a Monte Carlo code developed by the Kent State group.[16] An experimental check of the efficiency was obtained using the ^{3}He$(\pi^-, n)d$ reaction at angles that gave monoenergetic 150-MeV neutrons in coincidence with deuterons through LAS. By comparing singles in LAS to coincidences, an efficiency of 19.5±2 % was determined for a double-layered bar as compared to a calculated efficiency of 21%. Overall, the Monte Carlo calculations are believed to determine the neutron efficiency to an accuracy of better than 10%.

When neutrons were being detected in the bars, there was a significant chance of simultaneous signals in two bars from a charged particle going from one bar to another and, to a lesser extent, neutrons being scattered from one bar to another. For the double-layered bars, as many as 40% of the events were such double hits. For events in which there were signals within 2 nsec in both a front and a back bar, only the front-bar signal was used in the analysis. Events where adjacent bars showed hits were distributed evenly between the two.

Plastic paddles (VC, VNC), 55 cm×55 cm×6.3 mm, were placed halfway between the target and the arrays. The paddles covered the same solid angle as the arrays. For π^+ absorption, a software cut was placed on the pulse-height spectrum from the paddles so that only protons and more heavily ionizing particles were accepted, thus eliminating a large number of pions from knockout reactions. For π^- absorption, the paddle was used to veto all charged particles which, again, were mainly scattered pions. The blanking time of the veto was set so as to reject particles with $\beta (= v/c)$ ranging from 0.25 to 1. The deadtime introduced by this veto ranged from about 10% when the bars were forward to about 3% when they were at large angles.

The master trigger activated reading all of the digital signals which were than put on to tape. The data-acquisition computer was operated in the "may process" mode, which allowed on-line analysis when the computer was not busy writing events to tape.

III. DATA ANALYSIS

A cut was placed on the particle trajectories to eliminate events that did not originate in the target. Figure 2 shows a two-dimensional histogram of the time of flight through LAS vs the fractional momentum $\delta = (p - p_0)/p_0$; it can be seen that protons could be isolated by placing a cut on this two-dimensional histogram. Figure 3 shows a two-dimensional histogram of the time of flight to the bars versus proton momentum in LAS when π^+ absorption was being studied. When the final state consists of three nucleons, it is specified by nine quantities which are the three momentum components of each of the three nucleons. Conservation of energy and momentum reduces the number of independent variables to five. In the present work the five quantities that were mea-

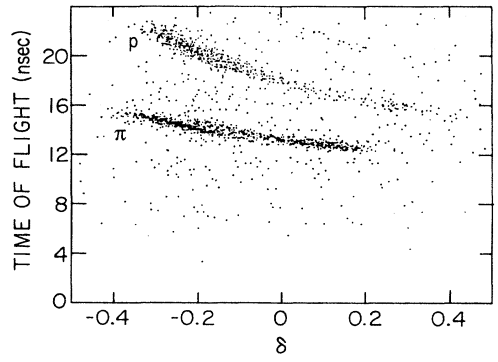

FIG. 2. Time of flight through LAS as a function of the fractional momentum, δ, where $\delta = p/p_0 - 1$. The pions and protons stand out clearly and, in the analysis, a cut was placed around the protons.

sured were the three components of the momentum of the proton that entered LAS and the two directional angles of the nucleon that hit the bars. The measurement of the time of flight to the bars provided additional information which was useful for eliminating background.

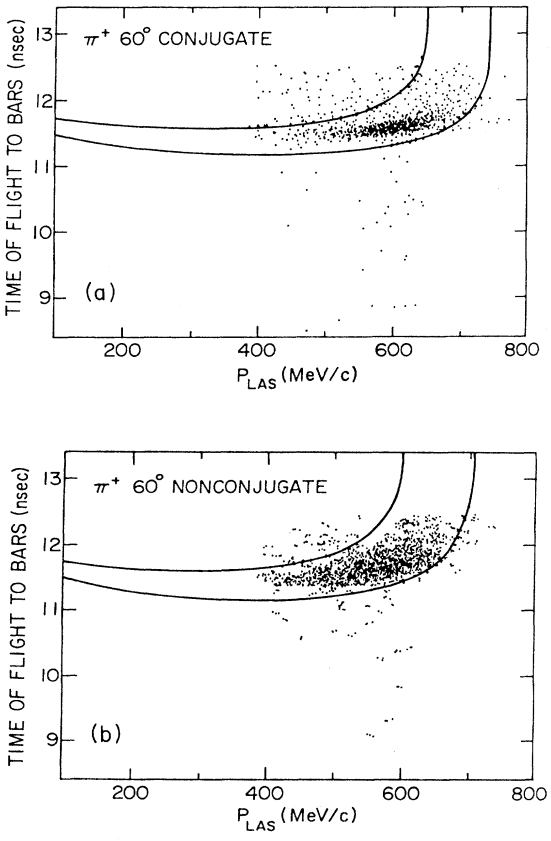

FIG. 3. Two-dimensional histograms of time of flight to the plastic bars versus proton momentum in LAS for π^+ absorption for (a) the conjugate array and (b) the nonconjugate array. The solid lines delineate the allowed region for three-body events. These data were taken with LAS at 60°.

The allowed region for three-body events is shown in Fig. 3. In determining this allowed region, the angular acceptances of LAS and the bars, the momentum resolution of LAS, and the time-of-flight resolution have been taken into account. When analyzing the data, a cut was placed that required the events to be in the allowed three-body region. Because the cut varied little from bar to bar within a given array, each array was treated as a single detector in placing this three-body cut. It is clear from Fig. 3 that there is a concentration of events within the three-body cut with, as expected, the concentration being more pronounced in the conjugate array than in the nonconjugate array, as seen in Fig. 3.

It is also clear that there is a background which, from its time distribution, appears to consist mainly of random coincidences. Randoms were determined by taking a cut similar to the three-body cut, but displaced in time so that truly coincident particles would have to be unphysical (i.e., traveling faster than the speed of light). For π^+ absorption, the randoms were only a few percent of the counts within the three-body cut for the conjugate array. For the nonconjugate array, the randoms were usually less than 10%, but, when LAS was at a backward angle, the nonconjugate randoms were sometimes as much as 30%. Empty-target backgrounds were measured at every angle. This background was small, usually less than 1%. When LAS was forward of about 40°, proton knockout was observed with the proton detected by LAS and the pion by the bars. The vast majority of these events did not pass the three-body cut; but, at the most forward LAS angles, the knockout was so intense that a significant number of these quasifree scattered pions were traveling slowly enough so as to spill into the three-body region. Because pions with the same velocity as protons have a much smaller range, these unwanted pions were rejected by requiring that the particle reach the back bars.

The 60° LAS momentum spectra for π^+ absorption are shown in Fig. 4. The three-body cut has been applied, and randoms have been subtracted, as has the empty-cell background. While the peak from two-body absorption dominates the spectrum in coincidence with the conjugate array, some correction had to be made for three-body absorption events which lie under the two-body peak. This correction was particularly important in the case of π^- absorption. The correction was made by assuming that the nucleon spectrum from three-body absorption is proportional to three-body phase space, and finding the proportionality constant from a region of nonconjugate array events where the number of two-body events would be negligibly small (i.e., at bar angles and LAS momenta far away from the two-body peak).

In arriving at the two-body absorption cross sections, a small correction was made for events that missed the conjugate array. This correction was calculated under the assumption that the angular correlation between the LAS proton and the nucleon into the bars was a Gaussian whose width was determined by the Fermi momentum of a nucleon in ^{3}He, as measured in electron scattering.[17] Because the total momentum of the three nucleons in ^{3}He

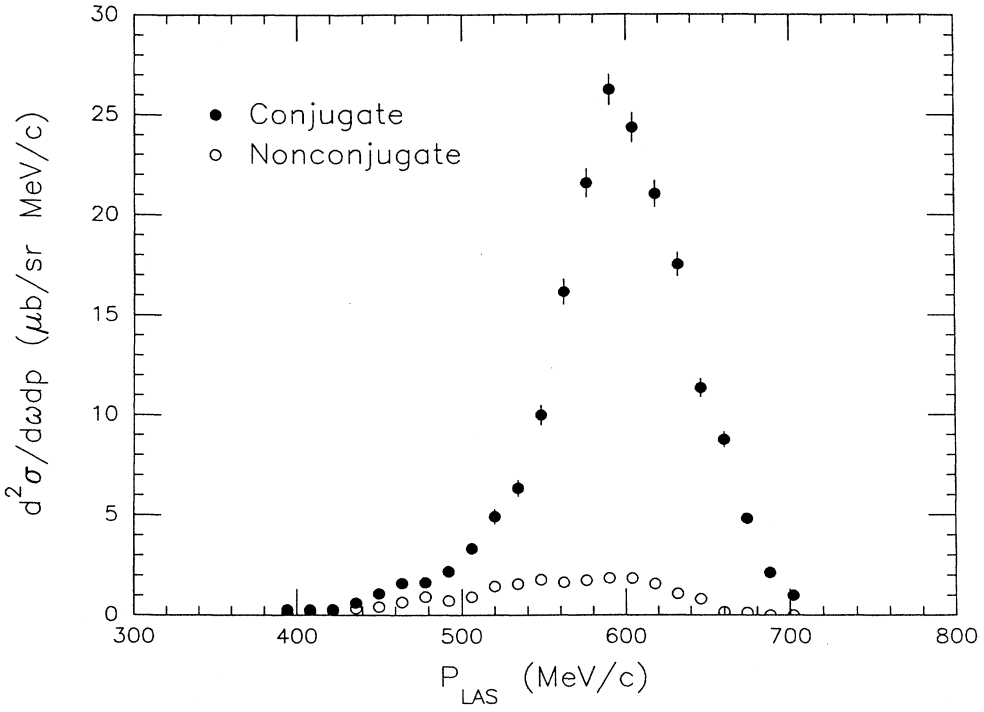

FIG. 4. LAS proton momentum spectra in coincidence with the plastic bars for π^+ absorption at $\Theta_{LAS}=60°$.

must be zero, the momentum of the absorbing pair is equal and opposite to that of the other nucleon. From the calculations, it was estimated that the fraction of events missed varied from about 1 to 2.3 %.

Data were taken in two runs a year apart. Several points were taken on both runs for both π^+ and π^- absorption, and whenever a point was repeated, the two values agreed to within 15%.

Two-dimensional histograms of time of flight to the bars vs LAS momentum for π^- absorption are shown in Fig. 5. The π^- data were more difficult to obtain for several reasons. First, the π^- flux was lower by about a factor of five. Second, the bars were only about 20% efficient as neutron detectors as against 100% efficient as proton detectors. Finally, the two-body absorption producing a charged particle, which accounts for the bulk of observed π^+ events, is more than an order of magnitude weaker for π^-. Nevertheless, the events from ^{3}He do stand out in the conjugate array two-dimensional histogram, whereas, for the nonconjugate array, even though the true to random ratio is clearly much smaller than it is for π^+, there is a distinct excess of events within the three-body cut. At 60° (Fig. 5), there were about three times as many nonconjugate coincidences within the three-body region as in the equivalent where only randoms were present.

The π^- data were analyzed in much the same way as the π^+. Figure 6 shows LAS spectra in coincidence with the conjugate and the nonconjugate arrays. For the conjugate array, randoms were about 20% when LAS was at a backward angle and could be as much as 50% when LAS was forward. The peak from two-body absorption stands out clearly though this mode cannot account for the entire spectrum. For the spectrum in coincidence with the nonconjugate array, randoms averaged about 30% of the counts within the three-body cut. The $\pi^- + pp \rightarrow p + n$ yield was obtained from the peak in the spectrum in coincidence with the conjugate array after estimating the three-nucleon absorption background in the manner described above. At 60° the error in the area of the peak is rather large, $\approx \pm 40\%$, as the π^- two-proton absorption is near a minimum (Fig. 8 below).

IV. RESULTS

A. Two-nucleon absorption

Differential cross sections for two-body π^+ absorption in the πNN center-of-mass system are plotted in Fig. 7. The total cross section is one-half of the integral of the differential cross section because the reaction produces two identical protons. As expected, the angular distribution is symmetric about 90°. Also shown in Fig. 7 are Legendre-polynomial fits to the data with two coefficients (A_0 and A_2), three coefficients (A_0, A_2, and A_4), and the $\pi^+ + d \rightarrow p + p$ angular distribution. The scaled $\pi^+ + d \rightarrow p + p$ angular distribution ($A_2/A_0 = 0.90 \pm 0.10$,

TABLE I. Coefficients found in fitting the differential cross sections for the $\pi+2N\rightarrow NN$ component of the $\pi+{}^3\mathrm{He}\rightarrow 3N$ reaction to $d\sigma/d\Omega=\sum_n A_n P_n(\cos\theta)$, where θ is the angle in the πNN system of the proton detected by LAS. For the present work, the listed errors on the Legendre coefficients are statistical only; the systematic errors are negligibly small. The total cross sections include a systematic uncertainty of about 15%. The total cross section is $\frac{1}{2}4\pi A_0$ for two-body π^+ absorption on a *pn* pair while, for π^- absorption on a *pp* pair, it is $4\pi A_0$.

	π^+		π^-			
T_π (MeV)	$\sigma\pm\delta\sigma$ (mb)	A_2/A_0	$\sigma\pm\delta\sigma$ (mb)	A_1/A_0	A_2/A_0	Reference
62.5	10.2±0.9	1.14±0.10	0.70±0.04	−0.82±0.13	1.62±0.13	6
64	10.4±1.6	1.17±0.06	0.53±0.10	−0.90±0.05	1.40±0.15	7
82.8	13.5±1.3	1.10±0.07	0.92±0.06	−0.79±0.12	1.68±0.16	6
119	17.3±2.0	1.10±0.06	1.08±0.16	−0.77±0.15	1.44±0.09	8
162	19.7±2.9	1.17±0.10	0.85±0.17	−0.69±0.04	1.94±0.11	8
165	17.0±2.6	1.01±0.09	0.91±0.20	−0.76±0.14	1.37±0.17	present work
206	13.0±1.7	1.33±0.10	0.92±0.18	−0.19±0.05	1.64±0.12	8
350	2.19±0.19		0.60±0.20	−1.21±0.21	2.30±0.23	11,18
500	0.72±0.07					11

$A_4/A_0=-0.21\pm0.05$) gives a satisfactory fit, reduced $\chi^2=1.35$, with a scaling factor of 1.45±0.17. If all three coefficients are allowed to vary, values of $A_2/A_0=0.45\pm0.23$ and $A_4/A_0=-0.78\pm0.22$ are obtained and the reduced χ^2 is lowered to 0.21. The main reason for needing a large A_4 is the most forward-angle data ($\theta_{\mathrm{LAS}}=30°$) and it is felt that the disagreement is not sufficient to permit the conclusion that the angular distribution from pion absorption on a $T=0$ pair in ^{3}He differs significantly from that from absorption on the deuteron. On the other hand, the two-coefficient fit is sufficiently poor, reduced $\chi^2=3.23$, that it appears likely that some A_4 is required.

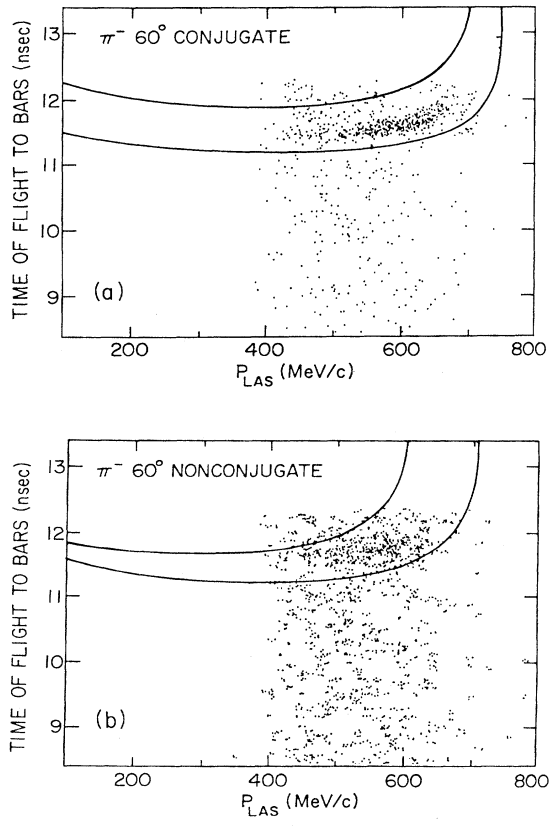

FIG. 5. Same as Fig. 3, but for π^- absorption.

Differential cross sections for π^- absorption on a *pp* pair are shown in Fig. 8. There is a strong backward asymmetry, as is also seen at both lower[6,7] and higher[18] energies. Also shown in Fig. 8 are the results of a three-coefficient (A_0, A_1, and A_2) and a four-coefficient (A_0, A_1, A_2 and A_3) fit. Three terms give a satisfactory fit, reduced $\chi^2=1.26$; if a fourth term is included, the reduced χ^2 decreases to 0.63. Again, it is the cross section at the most forward angle that brings about the need for the higher-order polynomial and, again, it is felt that this need is not definitely established. In any event, the π^- absorption cross section on a *pp* pair is about 5.5 that for two-body π^+ absorption.

The Legendre-polynomial coefficients that have been found at the various energies are tabulated in Table I. In order to facilitate comparison, the coefficients listed for the present work are those that only include terms through P_2 as these are the only terms that have been included at the other energies.

B. Three-nucleon absorption

As implied above, for both π^+, and π^- absorption, there is far more yield at nonconjugate angles than can be explained by absorption on a pair of nucleons. The momentum distribution of the nucleons in ^{3}He has been measured in electron-scattering experiments[17] and cannot account for the yield far from the two-body peak; therefore, it appears that in a significant fraction of events all three nucleons participate in the absorption. It has long been known that multinucleon absorption plays a major role in pion absorption in heavier nuclei[13] and the presence of a three-nucleon component in pion absorption by

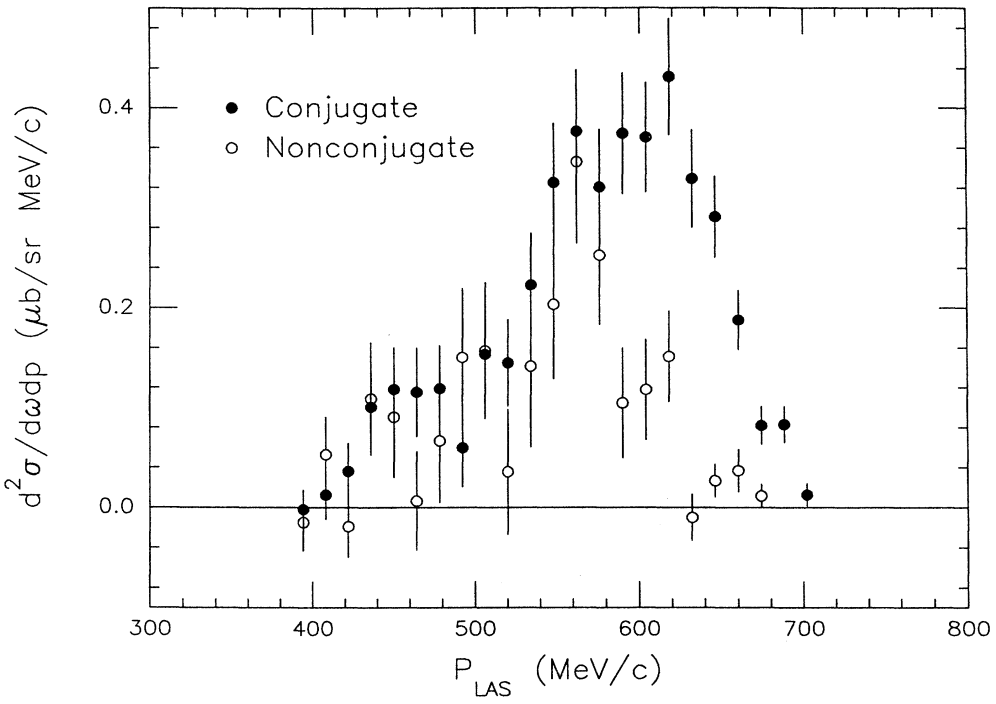

FIG. 6. Same as Fig. 4, but for π^- absorption.

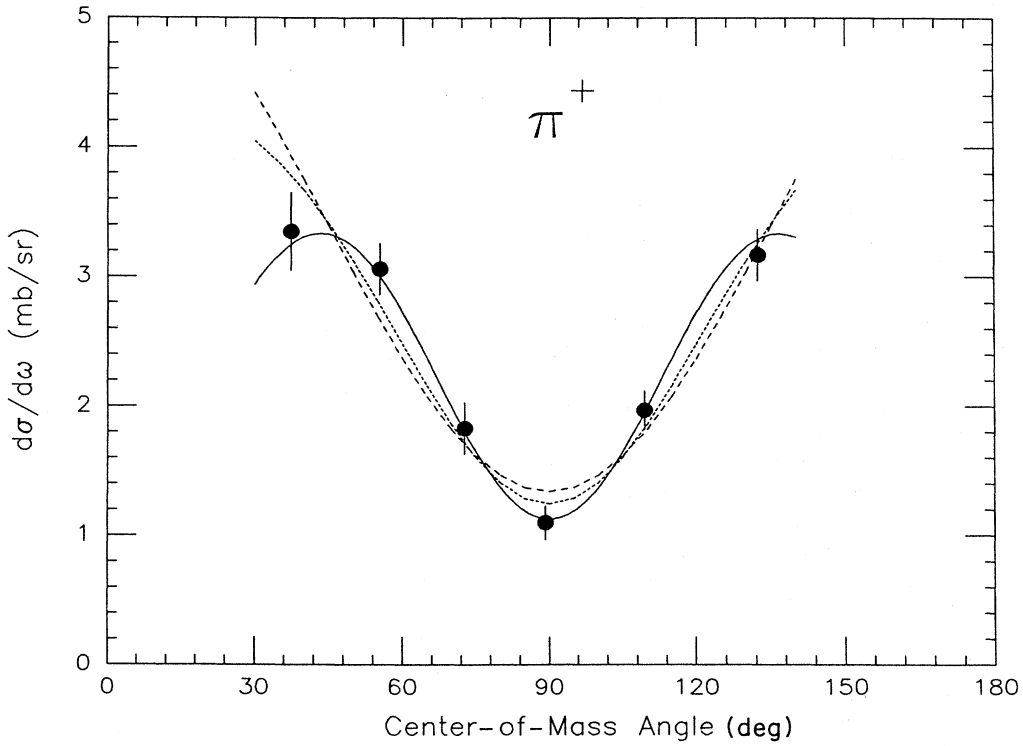

FIG. 7. Differential cross sections in the πNN system for π^+ absorption on a (p,n) pair. The errors include the uncertainty in the background, from three-body absorption, under the two-body peak. The overall 15% systematic uncertainty in absolute normalization is not included. The solid line is a three-coefficient Legendre polynomial fit ($A_0=2.33$, $A_2=1.05$, $A_4=-1.81$) to the data, the dashed line a two-coefficient fit ($A_0=2.71$, $A_2=2.74$), and the dotted line a fit ($A_0=2.61$, $A_2=2.32$, $A_4=-0.55$) which scales the $\pi^+ + d \rightarrow p + p$ angular distribution.

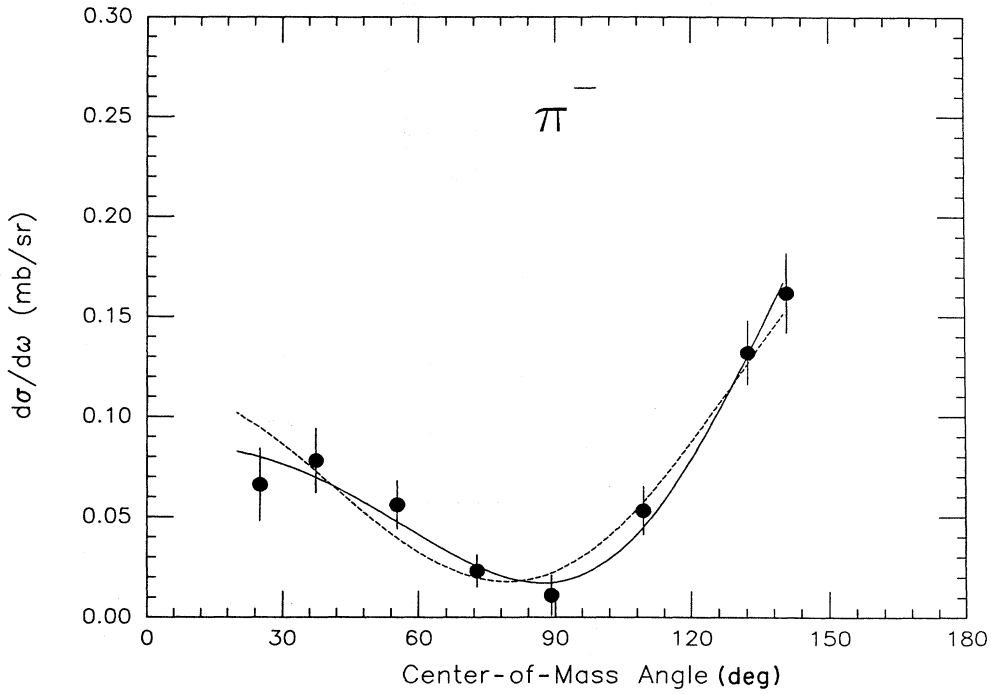

FIG. 8. Differential cross section as a function of proton angle for π^- absorption on a pp pair. At most angles, the major contributor to the stated error is the uncertainty in the background subtraction. The solid line is a four-coefficient fit ($A_0=0.074$, $A_1=-0.066$, $A_2=0.113$, $A_3=-0.033$) to the data and the dashed line a three-coefficient fit ($A_0=0.072$, $A_1=-0.055$, $A_2=0.099$).

^{3}He has been reported at energies below[6,9] and above[11] the Δ resonance.

The best place to observe three-body absorption appears to be in the momentum spectrum of the unobserved particle because the expected spectrum from two-body absorption is just that measured in electron scattering from ^{3}He. The momentum p_3 of the third, undetected, particle was calculated from (1) the momentum and direction of the particle in LAS, and (2) the scattering and azimuthal angles of the second particle as measured by the plastic bars ($\Theta_{\rm bar}$,$\Phi_{\rm bar}$).

The time resolution of about 250 psec in the measurement of the time of flight to the bars produced an error of $\sim$35 MeV/c in the measurement of the magnitude of the bar particle momentum. This error was too large to make the measurement useful in calculating p_3. The azimuthal angle $\Phi_{\rm bar}$ was determined from the time difference between signals from the top and bottom of a bar, while the bar position fixed $\Theta_{\rm bar}$ to $\pm 3.5°$ ($\pm 7°$ for 50.8-cm-wide bar). A spectrum of p_3 vs TOF$_{\rm bar}$ was created for each of the bars in order to determine the contribution from random coincidences. The locus of true ^{3}He events is a line broadened by the time and angular resolution of the detectors giving rise to a three-body cut similar to the one described above used on the $p_{\rm LAS}$ vs TOF$_{\rm bar}$ spectra. Spectra of random events were generated from the region outside of the cut in much the same manner as in the case of $p_{\rm LAS}$ vs TOF$_{\rm bar}$. Because the measurements were kinematically complete, $p_{\rm bar}$ was known for each event and each event was corrected for the efficiency of the bars as well as the acceptance of LAS. Finally, the spectra from the various bars were added in order to create a spectrum of $d^2\sigma/dp_3 d\Omega_1$ vs p_3 at each angle of LAS. A p_3 spectrum resulting from π^+ absorption is shown in Fig. 9 and one from π^- absorption is shown in Fig. 10.

For small values of p_3, particle 2 will be close to the conjugate direction; therefore, all events will be intercepted by the conjugate array. As p_3 is increased, events start to miss the conjugate array and the effective solid angle falls below $4p$. The unobserved particle momentum at which events start to be missed was 110 MeV/c when LAS was at 20° and increased to 150 MeV/c at the most backward angle of 130°.

The p_3 momentum spectrum would be expected to contain two components; one from two-body absorption and one from three-body absorption. In two-body absorption, the unobserved particle acts as a spectator and its momentum distribution may be expected to follow that obtained in exclusive electron scattering.[17] Such events dominate the low-momentum portion of the spectra and, as noted above, virtually all of them were detected by the conjugate array.

Where p_3 is great enough so that events can escape detection, the effective solid angle for three-body absorption is dependent on the distribution of events in phase space. In the present work, a matrix-element constant in phase space was assumed, and a calculation of the

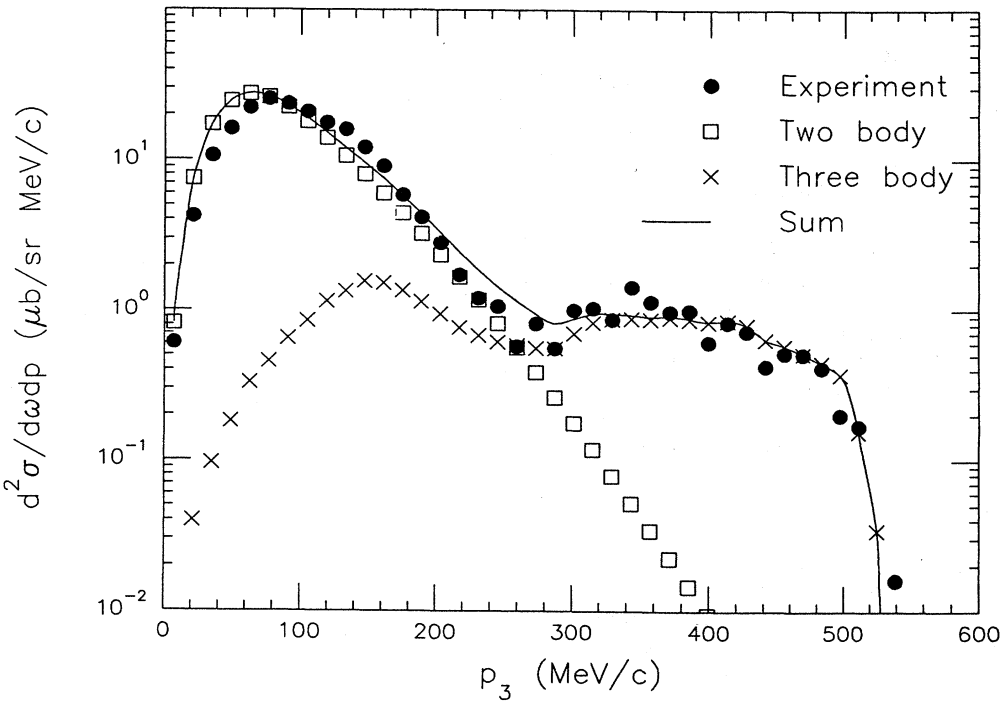

FIG. 9. Unobserved particle-momentum spectrum for π^+ absorption at $\Theta_{LAS}=120°$. The crosses are the predicted spectrum for a matrix-element constant in phase space and are postulated to have the shape of the three-body component. The open squares are the proton momentum distribution in ^{3}He as measured by electron scattering (Ref. 17) which is expected to have the shape of the two-body component. The magnitude of the two- and three-body components are adjusted to best fit the data, and the solid line is the sum of the two.

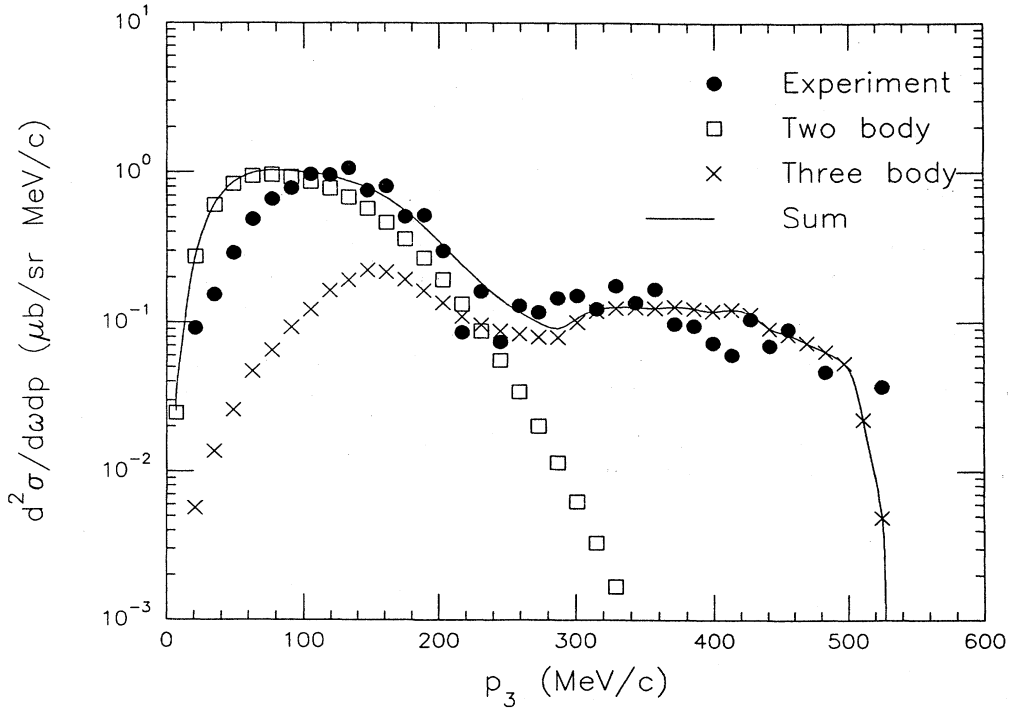

FIG. 10. Same as Fig. 9 for π^- absorption.

effective solid angle as a function of p_3 under this assumption is given in the Appendix.

Unobserved particle momentum distributions expected for (a) two-body absorption where the unobserved particle is a spectator, and (b) three-body absorption with a matrix-element constant in phase space are shown in Figs. 9 and 10 along with the data. The magnitude of the two components are adjusted to best fit the data. In analyzing their ^{3}He$(e,e'p)$ data, Jans *et al.*[17] separate the proton momentum distribution corresponding to the residual (pn) pair in the $(T=0)$ deuteron ground state from that forming a continuum extending up to leaving the (p,n) pair unbound by 14 MeV. Most of the yield in the continuum leaves the (p,n) pair unbound by 0–6 MeV, where the $2N$ system is primarily $T=1$, $S=0$. The momentum distribution leaving a $T=1$ pair was used in fitting the p_3 spectra from π^- absorption, and that leaving a $T=0$ pair for the spectra from π^+ absorption. The low-energy momentum distribution of the unobserved particle from π^+ absorption is in excellent agreement with that derived from electron scattering; whereas, in the case of π^- absorption, the agreement is not as good because the data are statistically poorer and because the momentum distribution from electron scattering could contain some contamination from residual $T=0$ states. The p_3 spectra were fitted to an incoherent sum of the momentum distributions expected for two-body and for three-body absorption and, as can be seen from Figs. 9 and 10, the fits were quite satisfactory. The differential cross sections for two-body absorption that were obtained from this fit agreed with those obtained from the peak in the LAS spectrum in coincidence with the conjugate array.

The observed cross section for π^+ absorption has to be divided by 3 in order to account for the fact that any one of the three protons can be detected by LAS. No such correction is needed for π^- absorption because there is only one proton in the final state. The three-body absorption cross sections that were obtained from the fit of the tw- and three-body components to the unobserved particle spectra are given in Table II. Statistical errors are no more than about 10% and there is, as in all of this work, a 15% systematic uncertainty in the overall normalization. A uniform population of phase space requires that the angular distribution follow three-body phase space; it can be seen from Table II that the deduced cross sections are roughly independent of angle. The variation of deduced three-body cross section with angle implies an uncertainty of about $\pm 25\%$ in the three-body cross section. This uncertainty is systematic and can be expected in all similar determinations of the three-body absorption cross section.

TABLE II. Cross sections for three-body absorption at 165 MeV obtained by fitting the unobserved particle momentum spectra to a two-body and a three-body component (Figs. 9 and 10). In calculating the total cross section for π^+ absorption, the fact that any of the three protons can be detected by LAS has been allowed for. Errors are discussed in the text. Three-body absorption cross sections have been reported for π^+ at 120 MeV by Backenstoss *et al.* (Ref. 19), and at 62.5 and 82.8 MeV for both π^+ and π^- by Aniol *et al.* (Ref. 6). An error has been found (Ref. 20) in the Aniol *et al.* analysis which lowers their published results by about a factor of 2. The present group has reported π^+ absorption cross sections at 350 and 500 MeV (Ref. 11). The results that have been obtained at the various energies are listed in Table III. The cross sections at 62.5 and 82.8 MeV are the corrected (Ref. 20) ones of Aniol *et al.* (Ref. 6).

	σ (mb)	
Θ_{LAS} (deg)	π^+	π^-
30	9.5	4.5
45		4.0
60	13.0	5.5
75	8.5	3.4
95	8.7	2.2
120	10.8	4.3
130		4.7

V. DISCUSSION

A. Two-nucleon absorption

Differential cross sections for two-body π^+ and π^- absorption in ^{3}He were recently reported[8] for a bombarding energy of 162 MeV, which is very near to that of the present work. The major difference between the two experiments is the larger angular range covered by the present work. The present work covered the c.m. angular range of 25°–140° for π^- and 35°–130° for π^+, as compared to the 50°–115° range covered in Ref. 8. In the region of overlap the differential cross sections obtained in the two experiments are similar, though for π^- absorption Ref. 8 appears to show a somewhat deeper dip in the region near 90°. For π^+ absorption, the coefficients obtained in the two-coefficient fit are in line with those reported at other energies (Table I). Extension of the angular range has the advantage of becoming sensitive to higher partial waves and, as noted above, the fit to the angular distribution following π^+ absorption is significantly improved when a P_4 term is included. The present results, as well as all measurements reported at lower energies, yield a cross section close to 1.5 times that for absorption on the deuteron, though a slightly higher ratio of 1.65 was found[11] at 350 MeV and a still higher ratio of 1.9 at 500 MeV. A ratio of 1.5 is what would be expected from counting the number of $T=0$ p-n pairs in ^{3}He. Significant distortion of the incoming or outgoing waves would be expected to reduce this value, with the distortions expected to be greatest at the resonance. Therefore, it appears that these distortion effects are not severe.

The two-body π^- differential cross sections show the backward peaking that is observed at lower bombarding energies (Table I). Above the resonance, the picture is not as clear in that a more symmetrical distribution is reported at 206 MeV,[8] but at 350 MeV the distribution is again found to be strongly backward peaked.[18] More data in the energy region above the resonance would be very helpful. The backward peaking has not been reproduced by meson-exchange calculations[21] but is predicted in the calculation of Miller and Gal[22] for absorption by a

six-quark state. While this agreement cannot be taken as a confirmation of the six-quark absorption mechanism, there do seem to be indications that processes other than conventional meson exchange are taking place. It has been shown[10,24] that absorption on a $T=1$ nucleon pair is not mediated by the delta resonance and, as such, is more sensitive to short-range correlations. Introduction of these correlations, whether through quark degrees of freedom or by other descriptions, may be essential for understanding this process. A three-coefficient fit yields results that are similar to those previously reported.[8] However, the data at the extreme angles calls for the inclusion of a P_3 component.

B. Three-nucleon absorption

All of the three-body cross sections reported to date were obtained under the assumption that the matrix element is constant in phase space. However, as noted above, the present work, which covers a wide angular range, demonstrates that cross sections obtained under this assumption have an uncertainty of at least ±25%. For this reason, where the published errors are less than 25%, a larger is also given in Table III. It is these larger values that are plotted for the error bars in Fig. 11.

The π^- three-body absorption cross section is in line with the values reported at lower energies.[6,20] Below the resonance, the π^+ three-body absorption cross section is comparable to the π^- and shows no discernible trend with energy. It is, therefore, surprising that the π^+ three-body cross section rises by about a factor of 2.5 at the resonance. It does not seem likely that this rise is due to experimental error, because the two-body cross sections are in good agreement with those reported at a nearby energy[8] and in line with results obtained at lower and at higher energies (Table I). Before attempting to interpret the three-body absorption cross sections, it is necessary to consider the possible effects of initial- and

TABLE III. Cross sections for three-body absorption at various energies. The errors given in parentheses take into account the estimated ±25% uncertainty introduced by the assumption that the three-body absorption matrix element is constant in phase space. All of the two- and three-body cross sections reported to date are plotted in Fig. 11.

T_π (MeV)	π^+ (mb)	π^- (mb)	Reference
62.5	3.6±0.9	4.5±1.1	6,20
82.8	2.8±0.7	3.5±0.9	6,20
120	3.9±0.5 (1.0)		19
165	9.2±2.3	4.2±1.2	this work
350	1.8±0.16 (0.45)		11
500	0.64±0.08 (0.16)		11

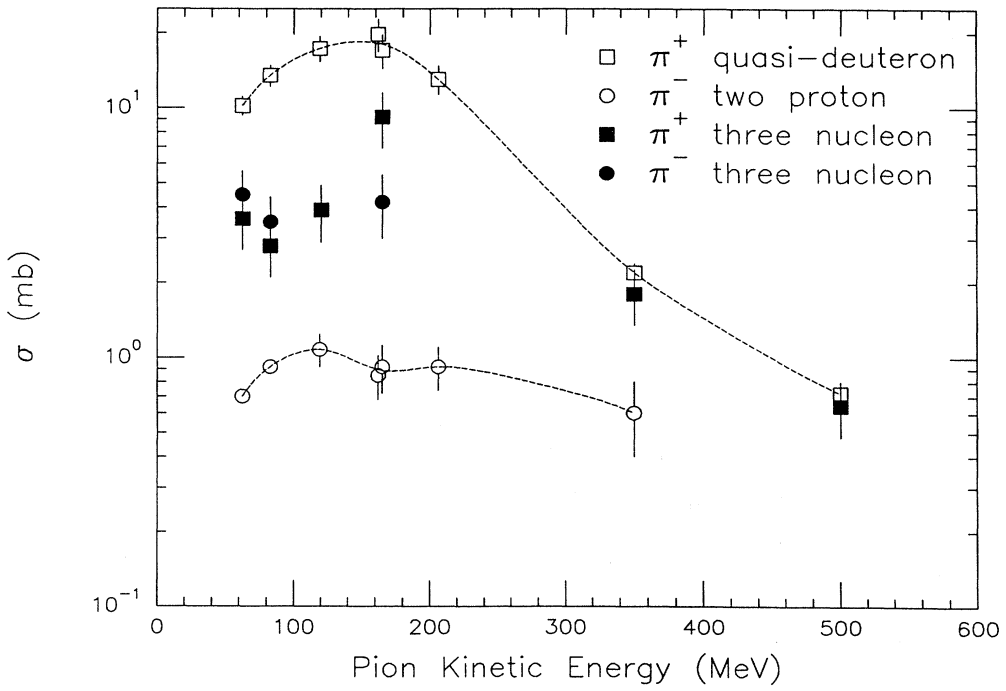

FIG. 11. Cross sections that have been reported for two-body (Table I) and three-body (Table III) absorption. The references are given in the tables. As noted in the text, the errors for the three-nucleon π^+ points at 120, 350, and 500 MeV have been increased to ±25%. The three-nucleon cross sections at 62.5 and 82.8 MeV have been corrected as reported in Ref. 21. The dashed lines are to guide the eye through the two-body points.

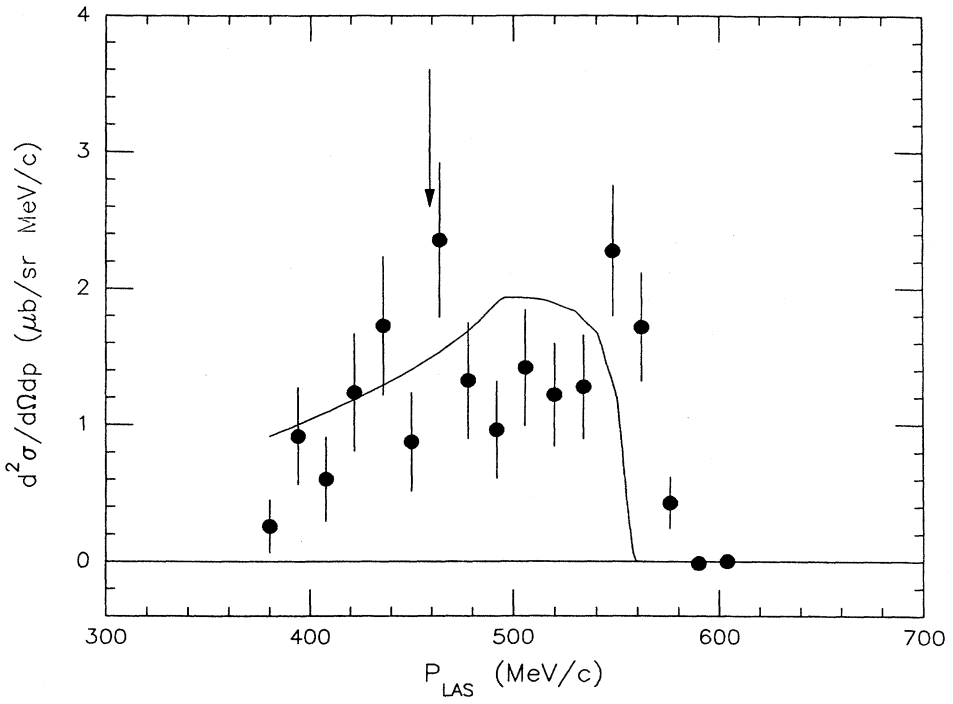

FIG. 12. Proton spectrum at 120° in coincidence with the nonconjugate array for π^+ absorption. The solid line is the spectrum expected for a matrix-element constant in phase space, normalized to the data over the entire momentum range. The arrow denotes the position of the two-body peak.

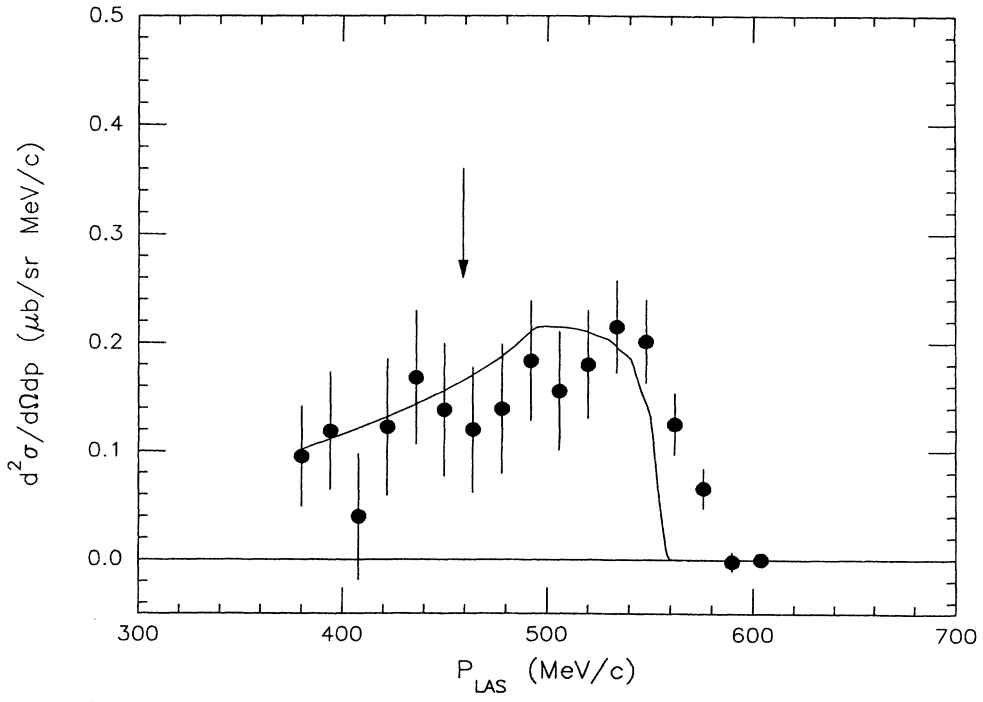

FIG. 13. Same as Fig. 12 for π^- absorption.

final-state interactions on two-body absorption.

Initial- and/or final-state interactions can lead to a sharing of the energy with a nucleon that is otherwise a spectator. In a final-state interaction, one of the nucleons would rescatter and the outgoing nucleons would no longer be at 180° in the πNN system. In the present experiment a signature of such events would be a coincidence between the nonconjugate array and LAS, with the LAS spectrum showing a peak at the momentum expected for two-body absorption (i.e., the spectrum in coincidence with the nonconjugate array would show a peak at the same place as the spectrum in coincidence with the conjugate array). However, the spectra shown in Figs. 4 (π^+) and 6 (π^-) show no such effect; the apparent peak in the spectrum in coincidence with the nonconjugate array shown in Fig. 6 is displaced by about 50 MeV/c from the position expected for a peak from final-state interactions. A somewhat better place to look is at backward angles as here the peak from two-body absorption is well below the momentum where the phase space goes through a maximum. The spectra at 120° in coincidence with the nonconjugate array are shown in Figs. 12 (π^+) and 13 (π^+). Clearly, any two-body peaks are but minor contributors to the spectra. Thus, final-state interactions do not appear to be responsible for a significant portion of the measured three-body absorption.

In an initial-state interaction the incident pion would scatter from a nucleon before being absorbed by an NN pair. Such interactions could not be responsible for a major portion of the π^- three-body absorption found in the present experiment because the protons detected by LAS would still have to come from absorption by the pp pair and this is a weak mode. There are also the protons from the initial-state scattering, but few of these would have sufficient momentum to be in the LAS acceptance window and, at any rate, π^--p scattering is relatively weak. However, in π^+ absorption, the protons from the absorbing pair could have been detected and, furthermore, the initial pion proton scattering would be much stronger. The pion's energy would be degraded in the initial scattering, leaving the πNN absorbing system with less momentum; in turn, this would mean that the NN correlation would be closer to 180° in the laboratory. Such an effect was sought by comparing the yield in the individual bars of the conjugate array, and looking for an asymmetry about 180° in the πNN system moving with the momentum of the incident pion beam. Results are shown in Fig. 14; there is no convincing evidence that the angular correlation between the two nucleons shows the effects of an initial-state interaction.

Salcedo *et al.*[23] have pointed out that a signature of the initial-state interaction described above would be a peak in the mass spectrum for the exchanged particle. The peak would be broadened because the pion is not on shell. When the off-shell effects are neglected, the invari-

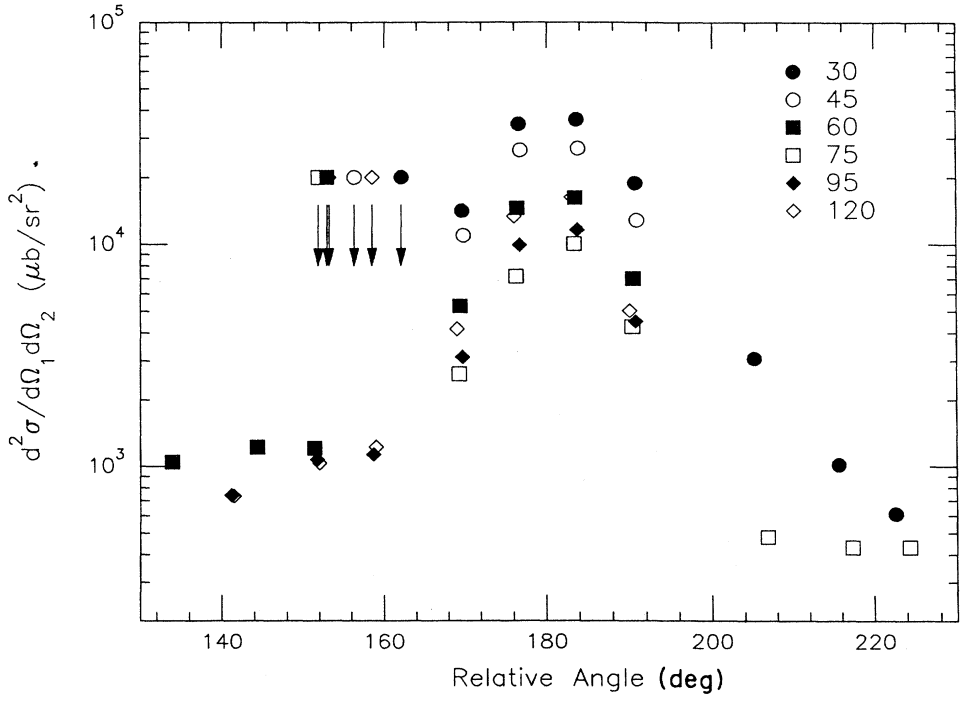

FIG. 14. Angular correlations between the two protons from π^+ absorption. The angles are in the laboratory system, except that 180 is the angle conjugate to LAS in the moving πNN system. The arrows represent the position of the peaks for pions absorbed at rest (i.e., 180° in the laboratory).

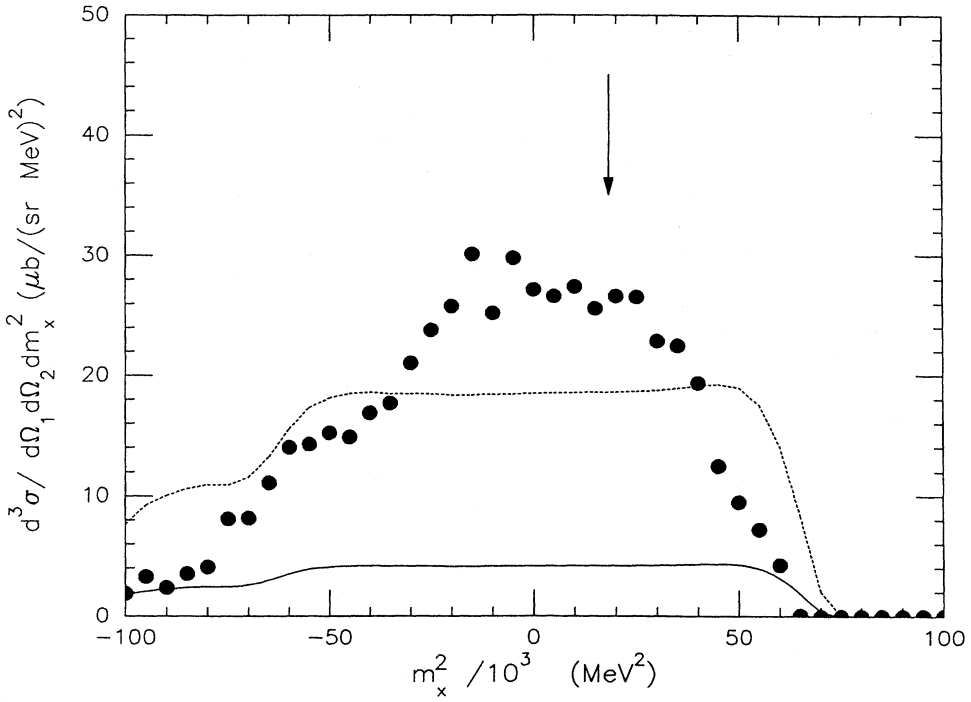

FIG. 15. Spectrum of m_x^2, where m_x is the mass of the exchanged particles as defined by Eq. (1) for coincidences from π^+ absorption with the conjugate array with LAS at 60°. The arrow is at m_π^2. The dotted line is the calculated spectrum for a matrix-element constant in phase space, normalized to the experimental spectrum over the entire m^2 range. The solid line is the same calculated spectrum but with the same normalization as that obtained for the nonconjugate array.

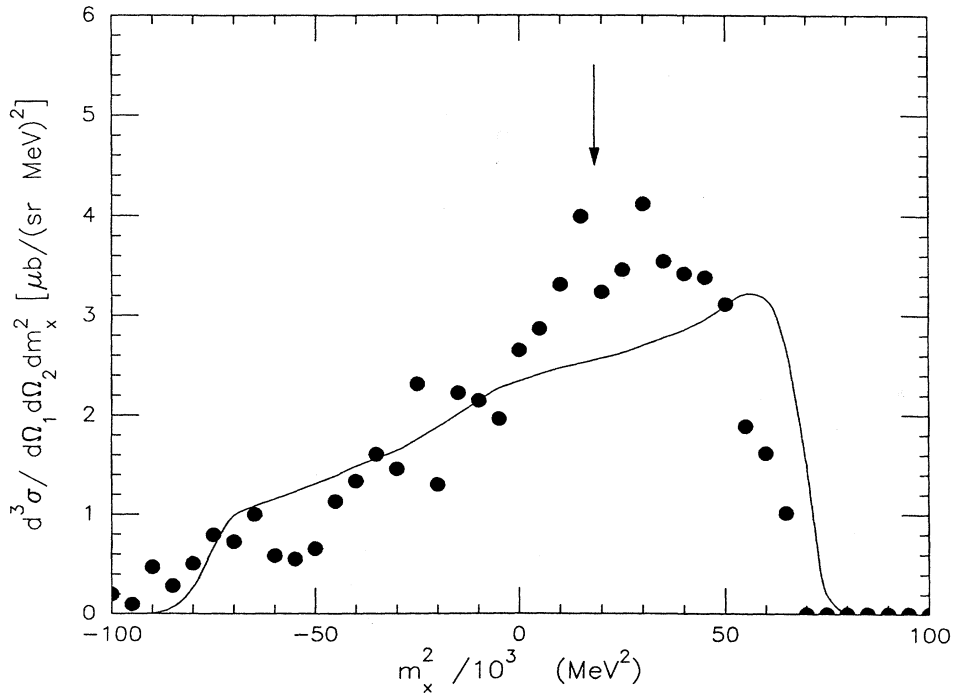

FIG. 16. Same as Fig. 15 but for the nonconjugate array.

ant mass of the exchanged particle is given by

$$m_x^2=(E-E_1-m_2-m_3)^2-(p-p_1)^2 , \quad (1)$$

where nucleon 1 is that struck in the initial interaction, after which the pion is absorbed by nucleons 2 and 3. It is, of course, not possible to tell *a priori* which of the protons is nucleon 1, therefore, for each event there are three different possible values for m_x^2.

The exchanged-particle spectrum accompanying two-body absorption (i.e., coincidences with the conjugate array) obtained with LAS at 60° is shown in Fig. 15 and that accompanying three-body absorption (i.e., coincidences between LAS and the nonconjugate array) in Fig. 16. For each event the value of m_x^2 near to 0 is chosen; the other possible values of m_x^2 are many m_π^2 away. It can be seen from Fig. 15 that, for two-body absorption, there is, indeed, a broad peak at about the expected position. From three-body absorption, Fig. 16, there is, at most, evidence for a small peak above the phase-space distribution in the right mass region. Similar m_x^2 spectra were found at the other angles.

Ashery[24] has speculated that a peak in the three-body cross section at the Δ resonance would be an indication of initial-state interactions. As noted above, such interactions cannot be significant in the observed π^- three-body cross section; however, they could be playing a role in the enhancement of the π^+ three-body cross section on resonance. The *p-p* angular correlations do not seem to support this contention; however, some evidence for initial-state interactions is found in the exchanged-particle spectra.

VI. CONCLUSIONS

Absorption of $\pi^+(-)$ by ^{3}He at the Δ-resonance energy of 165 MeV was studied by measuring proton-proton (proton-neutron) coincidences. Quasideuteron absorption, characterized by a sharp peak in the angular correlation of the outgoing particles, is clearly evident as is the component in which all three nucleons participate in the absorption process. The differential cross sections for π^+ absorption on a (pn) pair, $\pi^+ + {}^3\mathrm{He} \rightarrow (pp)+p$, are fitted well by $1.5(\pi^+ d \rightarrow p+p)$. The cross section for π^- absorption on a (pp) pair, $\pi^- + {}^3\mathrm{He} \rightarrow (pn)+n$ is about 5% that for absorption on a $T=0$ pair and peaked strongly in the backward (proton) direction. There appears to be little change in the asymmetry in going through the Δ resonance, though there is some experimental disagreement on this point. Absorption on a $T=0$ pair exhibits a strong peak at the Δ resonance, while there is no evidence of the resonance in the energy dependence of the absorption on a $T=1$ pair.

For both π^+ and π^- absorption, the momentum spectra of the unobserved particle agree well at low momenta with that found in electron scattering for the nucleons in ^{3}He but also contain a high-momentum portion that appears to be from three-body absorption. These spectra are fitted well by assuming a three-body matrix element that is constant over phase space; and the angular distributions are reasonably consistent with this assumption. For the π^+ reaction, three-body absorption is about one-third of the total absorption over the entire range for which measurements have been reported, 62–500 MeV. For the π^- reaction, three-body absorption is about 90% of the observed total below and at the Δ resonance with no data having been reported at higher energies. Final-state interactions do not appear to be contributing significantly to the observed three-body components. Initial-state interactions cannot be responsible for a significant portion of the observed π^- three-body cross section. The mechanism that causes the π^+ three-body absorption to peak at the resonance has not been identified, and it is possible that initial-state interactions play some role.

ACKNOWLEDGMENTS

This work was supported by National Science Foundation (NSF) Grants PHY-8911777 (Northwestern) and PHY-8802392-02 (Kent State), U.S. Department of Energy, Nuclear Physics Division, under Contracts W-31-109-ENG-38 (Argonne) and DE-AS05-726ER0403 (Virginia), and the U.S.-Israel Binational Science Foundation (Tel-Aviv).

APPENDIX: CALCULATION OF THE UNOBSERVED PARTICLE SPECTRUM

For three particles, x, y, and z, uniformly distributed in phase space,

$$\frac{d^3R}{dp_x d\Omega_x d\Omega_y} = \left| \frac{p_x^2 p_y^2}{(2\pi)^5 E_x [E_y p_y + E_z p_y - p_0 E_y \cos(\theta_y) + p_x E_y \cos(\theta_{xy})]} \right| , \quad (A1)$$

where p_0 is the incident pion momentum,

$$\cos\theta_{xy} = \cos\theta_x \cos\theta_y + \sin\theta_x \sin\theta_y [\cos(\phi_y - \phi_x)] .$$

Using this distribution, a Monte Carlo calculation was performed in order to determine the efficiency, as a function of momentum, for detecting the unobserved particle. This calculation was performed for each angle at which LAS was set. In the calculation, the direction of one of the particles (θ_y, ϕ_y) was fixed (i.e., particle y enters LAS) and the momentum and direction of another particle (p_x, θ_x, ϕ_x) picked randomly. Because five variables have been chosen, the event is now kinematically complete and the other momenta and angles can be calculated. In doing so, a quadratic equation for the momentum p_y must be solved; there are two solutions, one or both of which can be negative, and those events with negative p_y are discarded. Each event is then weighted by the magnitude of the phase-space element given in Eq. (A1).

Histograms of spectra of the unobserved particle are incremented for events in which p_y falls within the momentum acceptance of LAS and either particle x or z (a) is above the experimental threshold of 310 MeV/c and (b) hits either the nonconjugate or the conjugate array. A separate histogram is kept for each type of event (e.g., particle x in the conjugate array, etc.). Separate histograms are kept for the few ($< 1\%$) events where both particle x and z were detected. The calculated momentum spectrum of unobserved particles is made by adding the histograms.

This calculation was done for every angle at which LAS was set. As a check on the Monte Carlo calculation, for a particular setting of LAS the fraction of phase space intercepted by a particular array of detectors can be calculated by integrating the phase-space equation (A1) (putting in the appropriate momentum cuts) and comparing the fraction intercepted to that predicted by the Monte Carlo calculation. The Monte Carlo calculation was found to predict twice as many events, which is expected since the calculation permits either of the two nucleons not going into LAS to be counted. In fact, the Monte Carlo calculation finds the same (within statistics) unobserved particle spectrum when particle x is detected as when particle z is detected. The total predicted spectrum is the sum of the two.

---

*Present address: Bell Telephone Laboratories, Whippany, NJ 07981.

†Present address: Massachusetts Institute of Technology, Cambridge, MA 02139.

[1]C. Richard-Serre, W. Hirt, D. F. Measday, E. G. Michaelis, M. J. M. Saltmarsh, and P. Skarek, Nucl. Phys. **B20**, 413 (1970).

[2]B. G. Ritchie, G. S. Blanpied, R. S. Moore, B. M. Preedom, K. Gotow, R. C. Minehart, J. Boswell, G. Das, H. J. Ziock, N. S. Chant, P. G. Roos, W. J. Burger, S. Gilad, and R. P. Redwine, Phys. Rev. C **27**, 1685 (1983).

[3]R. D. Mckeown, S. J. Sanders, J. P. Schiffer, H. E. Jackson, M. Paul, J. R. Specht, E. J. Stephenson, R. P. Redwine, and R. E. Segel, Phys. Rev. Lett. **44**, 1033 (1980).

[4]A. Altman, E. Piasetzky, J. Lichtenstadt, A. I. Yavin, D. Ashery, R. J. Powers, W. Bertl, L. Felawaka, H. K. Walter, R. G. Winter, and J. V. D. Pluym, Phys. Rev. Lett. **50**, 1187 (1983).

[5]D. Gotta, M. Dorr, W. Fetscher, G. Schmidt, H. Ullrich, G. Backenstoss, W. Kowald, I. Schwanner, and H. J. Weyer, Phys. Lett. **112B**, 129 (1982).

[6]K. A. Aniol, A. Altman, R. R. Johnson, H. W. Roser, R. Tacik, U. Wienands, D. Ashery, J. Alster, M. A. Moinester, E. Piasetzky, D. R. Gill, and J. Vincent, Phys. Rev. C **33**, 1714 (1986).

[7]M. A. Moinester, D. R. Gill, J. Vincent, D. Ashery, S. Levenson, J. Alster, A. Altman, J. Lichtenstadt, E. Piasetzky, K. A. Aniol, R. R. Johnson, H. W. Roser, R. Tacik, W. Gyles, B. Barnett, R. J. Sobie, and H. P. Gubler, Phys. Rev. Lett. **52**, 1203 (1984).

[8]P. Weber, G. Backenstoss, M. Izycki, R. J. Powers, P. Salvisberg, M. Steinacher, H. J. Weyer, S. Cierjacks, A. Hoffart, H. Ullrich, M. Furic, T. Petkovic, and N. Simicevic, Nucl. Phys. **A501**, 765 (1989).

[9]G. Backenstoss, M. Izycki, P. Salvisberg, M. Steinacher, P. Weber, H. J. Weyer, S. Cierjacks, S. Ljungfelt, H. Ullrich, M. Furic, and T. Petkovic, Phys. Rev. Lett. **55**, 2782 (1985).

[10]D. Ashery, R. J. Holt, H. E. Jackson, J. P. Schiffer, J. R. Specht, K. E. Stephenson, R. D. Mckeown, J. Ungar, R. E. Segel, and P. Zupranski, Phys. Rev. Lett. **47**, 895 (1981).

[11]L. C. Smith, R. C. Minehart, D. Ashery, E. Piasetzky, M. Moinester, I. Navon, D. Geesaman, J. P. Schiffer, G. Stephens, B. Zeidman, S. Levenson, S. Mukhopadhyay, R. E. Segel, B. Anderson, R. Madey, J. Watson, and R. R. Whitney, Phys. Rev. C **40**, 1347 (1989).

[12]J. Kallne, R. C. Minehart, R. R. Whitney, R. L. Boudrie, J. B. McClelland, and A. W. Stetz, Phys. Rev. C **28**, 304 (1983).

[13]B. J. Dropesky, G. W. Butler, C. J. Orth, R. A. Williams, M. A. Yates-Williams, G. Friedlander, and S. B. Kaufman, Phys. Rev. C **20**, 1844 (1979).

[14]L. Orphanos, J. S. McCarthy, R. C. Minehart, P. A. M. Gram, B. Höistad, C. F. Perdrisat, and J. Källne, Phys. Rev. C **26**, 2111 (1982).

[15]E. Colton, Nucl. Instrum. Methods **178**, 95 (1980).

[16]R. A. Cecil, B. D. Anderson, and R. Madey, Nucl. Instrum. Methods **161**, 439 (1979).

[17]E. Jans, P. Barreau, M. Bernheim, J. M. Finn, J. Morgenstern, J. Mougey, D. Tarnowsky, S. Turck-Chieze, S. Frullani, F. Garibaldi, G. P. Capitani, E. de Sanctis, M. K. Brussel, and I. Sick, Phys. Rev. Lett. **49**, 974 (1982).

[18]L. C. Smith, R. Minehart, D. Ashery, E. Piasetzky, M. Moinester, I. Navon, D. Geesaman, J. P. Schiffer, G. Stephans, B. Zeidman, S. Mukhopadhyay, R. E. Segel, B. Anderson, R. Madey, and J. Watson, in *Proceedings of the Eleventh International Conference on Particles and Nuclei, Kyoto, Japan, 1987,* edited by S. Homma *et al.* (North-Holland, Amsterdam, 1988), p. 338; C. Smith, private communication.

[19]G. Backenstoss, M. Izycki, R. Powers, P. Salvisberg, M. Steinacher, P. Weber, H. J. Weyer, A. Hoffart, B. Rzehorz, H. Ullrich, D. Bosnar, M. Furic, and T. Petkovic, Phys. Lett. B **222**, 7 (1989).

[20]D. Ashery (unpublished).

[21]O. V. Maxwell and C. Y. Cheung, Nucl. Phys. **A454**, 606 (1986).

[22]G. A. Miller and A. Gal, Phys. Rev. C **36**, 2450 (1987).

[23]L. L. Salceodo, E. Oset, D. Strottman, and E. Hernandez, Phys. Lett. B **208**, 339 (1988).

[24]D. Ashery, Nucl. Phys. **A478**, 603c (1988).